Ka-Band Dual-Frequency Single-Slot Antenna Based on Substrate Integrated Waveguide

Wan Jiang, Kama Huang, and Changjun Liu, *Senior Member, IEEE*

***Abstract*—This letter presents a novel dual-frequency single-slot antenna in Ka-band based on a substrate integrated waveguide (SIW). From the view of an SIW resonator, the single-slot cuts currents of the TE_{101} and TE_{102} mode in two frequencies, respectively, which leads to a dual-frequency performance. In addition, the difference between two resonance frequencies may be tuned by varying the length of the SIW, which changes the resonant frequencies of the two modes. Three antennas operating from 25.3 to 30.7 GHz with gain greater than 6 dBi are designed and fabricated. Simulated and measured results of the antennas are presented as well. The results show that the proposed antennas achieve stable tunable dual-frequency performance, which may be applied to a Ka-band communication system.**

***Index Terms*—Dual-frequency, single-slot antenna, substrate integrated waveguide (SIW) resonator.**

I. Introduction

NOWADAYS, the millimeter-wave range wireless communication systems draw great attention in the industry and academia [1]–[5]. With the increasing demand in the mobile communication and the radar systems, compact and multiband antennas have great applications in such areas. Apart from that, the small wavelength in the millimeter-wave range enables small antenna dimensions, which make antennas being integrated in different circuits. Slot antennas are one of the most brilliant candidates in applications of the wireless communication and radar systems due to their low profile, good radiation efficiency, and simple structure [6]–[8]. To obtain the dual-frequency property into slot antennas, much research has been performed during the last decades [9]–[12]. The research has successfully realized the dual-frequency property with slots or complicated active components. The applications in the mobile communication and radar systems require more compact dual-frequency antennas.

Substrate integrated waveguide (SIW) structures have the advantages of low loss, easy integration, and high power capacity [13], [14]. With lower energy leakage and profile than microstrip lines and rectangular waveguides (RWGs), SIW structures have a promising application in the millimeter-wave range and the terahertz frequency. Moreover, it also has substantive applications in slot antennas within the millimeter-wave range, especially in the Ka-band frequency range.

Manuscript received November 6, 2017; revised November 27, 2017; accepted November 30, 2017. Date of publication December 8, 2017; date of current version February 5, 2018. This work was supported in part by the 973 program 2013CB328902 and in part by the defense industrial technology development program. *(Corresponding author: Changjun Liu.)*

The authors are with the School of Electronics and Information Engineering, Sichuan University, Chengdu 610064, China (e-mail: jiangwan_126@126.com; kmhuang@scu.edu.cn; cjliu@ieee.org).

Digital Object Identifier 10.1109/LAWP.2017.2781219

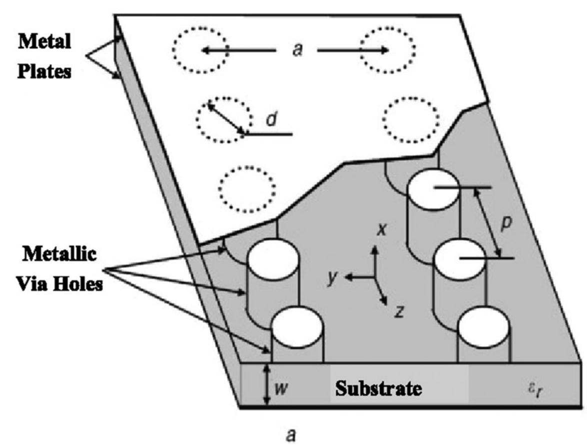

Fig. 1. Basic structure and parameters of the SIW.

In this letter, we demonstrate a novel technique to design dual-frequency single-slot antennas based on an SIW structure. The proposed dual-frequency single-slot antennas consist of an SIW structure, which can be regarded as a resonator, a slot, and a transition. Considering the first two modes (TE_{101} and TE_{102}) in the SIW resonator, the slot cuts currents of both modes to radiate energy into the free space, which has a good performance on two resonance frequencies. In the Ka-band, i.e., the frequency range between 26.5 and 40 GHz, two frequency bands have possible applications in mobile communication networks, Ka-band satellite-on-the-move communication terminal and fifth generation wireless communications in the future [15]–[17].

II. Theory and Design

A. SIW Resonator Analysis

As shown in Fig. 1, a conventional SIW structure has a dielectric substrate separating two metal plates, which are shorted by two rows of metallic via holes. The performance of the SIW structure is similar to the conventional RWG, which replaces the vertical metal walls by metallic via holes. To avoid the energy leakage from adjacent two vias, the rule $p/d < 0.25$ should be satisfied [13], where d is the diameter of vias, p is the distance between each via, and λ_g is the wavelength in the substrate. According to the parameters of the SIW structure, we can get the equivalent width a_{equ} and length l_{equ} of the conventional RWG

TABLE I
SIW STRUCTURE PARAMETERS AND CALCULATED RESONANT FREQUENCIES

SIW width (a)	4.41 mm	SIW length (l)	11.23 mm
Via diameter (d)	0.5 mm	Via distance (p)	0.7 mm
Equivalent width (a_{equ})	4.02 mm	Equivalent length (l_{equ})	10.82 mm
Resonance frequency f_1 (TE_{101})	26.91 GHz	Resonance frequency f_2 (TE_{102})	31.35 GHz

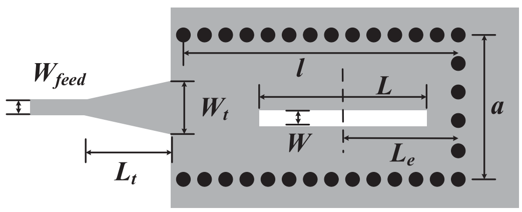

Fig. 2. Proposed dual-frequency single-slot antenna A.

[14]. Besides, the resonance frequency of the SIW resonator is

$$f\left(\mathrm{TE}_{m0q}\right) = \frac{c_0}{2\sqrt{\varepsilon_r}}\sqrt{\left(\frac{m}{a_{\mathrm{equ}}}\right)^2 + \left(\frac{q}{l_{\mathrm{equ}}}\right)^2} \qquad (1)$$

where c_0 is the speed of the light and ε_r is the dielectric constant of the substrate. The resonance frequencies of TE_{101} and TE_{102} modes of the SIW resonator are obtained from (1). The resonator is performed in the Rogers RT/Duroid 5880 with the substrate thickness of 0.254 mm and dielectric constant of 2.2.

Based on the theoretical calculation, the parameters of the SIW resonator and the resonance frequencies f_1 and f_2 of the TE_{101} and TE_{102} modes are depicted in Table I, where a is the distance between two rows of metallic via holes, i.e., the width of the SIW resonator, and l is the length of the SIW resonator. Besides, the length of the SIW resonator affects the resonant frequencies of two modes according to (1). It may be applied to adjusting the resonant frequencies and their difference of the proposed antenna. The theoretical calculation is the basis of the dual-frequency antenna design.

B. Antenna Design

Based on the theoretical calculation of the resonance frequencies of TE_{101} and TE_{102} modes of the SIW resonator, the proposed dual-frequency single-slot antenna A is presented in Fig. 2. Normally, for a dielectric-filled guide, the slot length can be approximated by $L = \lambda_o/\sqrt{2(\varepsilon_r+1)}$ [18], where λ_o is the wavelength at the resonance frequency of the slot. However, the slot length L of the proposed antenna should be chosen properly in the design to ensure that currents of both modes are disturbed at the same time. From the view of an SIW resonator, the length L should be calculated from the guided wavelength of f_2. The L is a little bit greater than the half-wavelength of f_2 to make sure the slot cuts the currents of two resonance frequencies. Besides, a tapered microstrip line transition is applied in the antenna A design due to its wide bandwidth, as shown in Fig. 2. The dimension of the transition is set to be: $W_{\mathrm{feed}} = 0.76$ mm, $L_t = 2.28$ mm, and $W_t = 1.32$ mm, while the dimension of the slot is $L = 5.66$ mm $= 6\lambda_g/10 \approx \lambda_g/2$ (λ_g is the guided wavelength of f_2), $l = 11.2$ mm, and $L_e = 5.37$ mm. Fig. 3 shows the electric fields of the proposed antenna A of f_1 and f_2 (TE_{101} and TE_{102}). There are strong electric fields around the slot at two frequencies of TE_{101} and TE_{102} modes, which create the radiation of the microwave energy. Compared with a pure SIW resonator, it can be seen that the electric field distribution of TE_{101} and TE_{102} modes match well. It should be noticed that the electric field distribution of TE_{101} mode is far from the input port of the SIW structure due to the input transition, which may affect f_1 (TE_{101}) of the proposed dual-frequency single-slot antenna. Fig. 4 presents the simulated comparison of input reflection coefficients ($|S_{11}|$) of antenna A, which has resonances at 25.8 and 31.5 GHz.

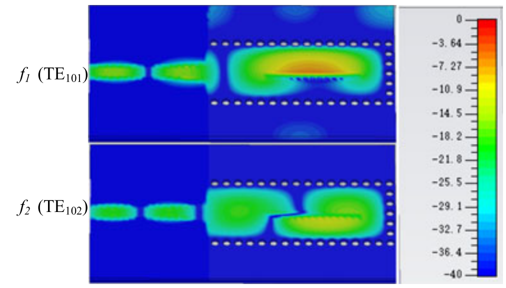

Fig. 3. Electric field distribution of the proposed antenna A of two modes on two resonance frequencies.

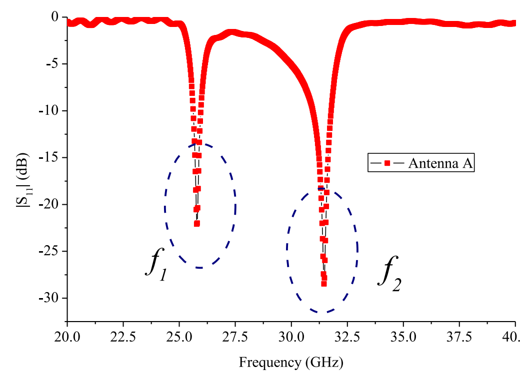

Fig. 4. Simulated comparison of input reflection coefficients ($|S_{11}|$) of antenna A.

Furthermore, the resonance frequencies and the frequency differences may be adjusted by changing the length, i.e., the equivalent length l_{equ}, of the SIW structure. According to (1), the resonance frequencies of TE_{101} and TE_{102} modes are affected by varying the SIW structure length, which makes the frequencies of the antenna adjustable. To verify the frequency adjustable property, two more antennas, antennas A_1 and A_2, are proposed, and their detailed dimensions are shown in Table II. The width of slots $W = 0.3$ mm. Combined with the variation of the length of the SIW structure, optimization of the slot dimensions, with the dimensions shown in Table II, means that the antenna resonance frequencies are adjustable. Fig. 5 shows the simulated input reflection coefficients ($|S_{11}|$) of proposed

TABLE II
DIMENSIONS OF DUAL-FREQUENCY ANTENNAS A, A_1, AND A_2

Parameters	Dielectric Substrate: RT/Duriod 5880 ($h = 0.254$ mm)			
	Symbol	Value (mm)		
		Antenna A	Antenna A_1	Antenna A_2
Slot length	L	5.66	5.99	5.92
SIW length	l	11.2	10.19	9.43
Slot location	L_e	5.37	5.27	5.2

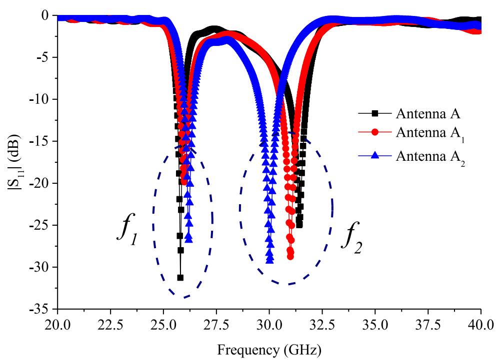

Fig. 5. Input reflection coefficients of antennas A, A_1, and A_2, which shows the possibility for frequency adjustment.

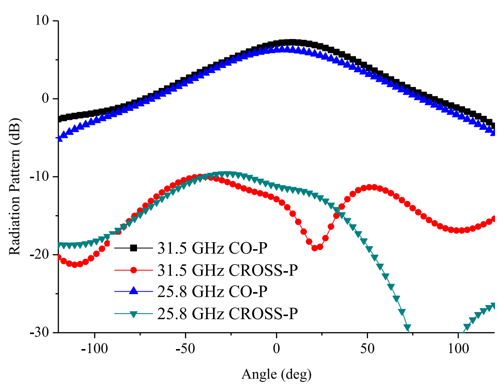

Fig. 6. Radiation pattern at 25.8 and 31.5 GHz of antenna A.

antennas A, A_1, and A_2. The three antennas resonate in the frequency range from 25.8 to 31.5 GHz.

However, the frequencies may be only tuned in a narrow range due to the limitation of the two modes of the resonator. Moreover, this dual-frequency property can only be realized in an SIW structure with a small length owing to the rapid attenuation of higher modes in the waveguide. As the consequence of it, only the first two modes can be utilized in this mechanism to realize a dual-frequency single-slot antenna.

The simulated and theoretical calculated results of antenna A agree well at f_2. However, the mismatch of the first resonance frequency may be caused by the influence of the input transition, which was not taken into account in the theoretical calculation as explained in the first paragraph of this part. Fig. 6 shows the radiation pattern including both copolarization and cross

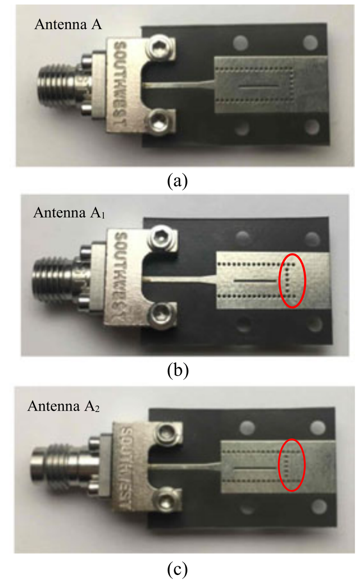

Fig. 7. Fabricated antennas: (a) the proposed dual-band antenna A, (b) and (c) the dual-band antennas A_1 and A_2 with shifted SIW length for frequency adjustment.

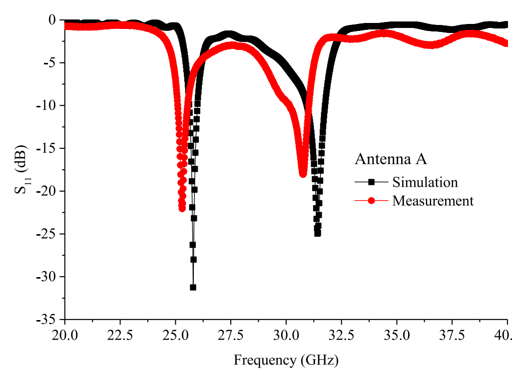

Fig. 8. Measured and simulated input reflection coefficients of antenna A.

polarization of two resonance frequencies of antenna A. The gain of each resonance frequency is 6.3 and 6.9 dBi, respectively. Due to the similar radiation property among antennas A, A_1, and A_2, only the radiation pattern of antenna A is presented.

III. ANTENNA FABRICATION AND MEASUREMENTS

The proposed antennas shown in Fig. 7 were fabricated and measured for verification using Rogers RT/Duroid 5880 substrate with thickness of 0.254 mm and permittivity of 2.2. Antennas A, A_1, and A_2 are designed to present the frequency adjustment property. The S-parameters were measured with an Agilent network analyzer E8363C. The comparison between simulated and measured S-parameters of antenna A are depicted in Fig. 8. A reasonable agreement has been achieved between measurement and simulation. The frequency shift between simulated and measured results is owing to the fabrication tolerance and dielectric constant of the substrate. As shown in Fig. 9, the fabricated antennas A, A_1, and A_2 resonate from

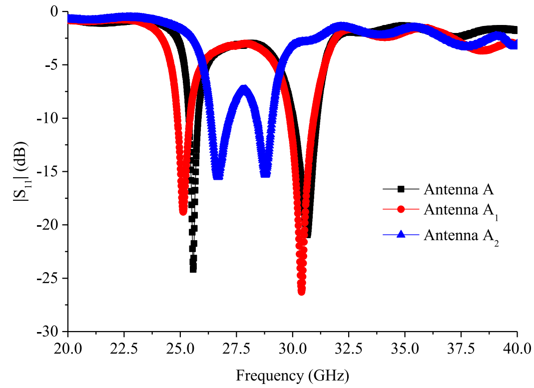

Fig. 9. Measured input reflection coefficients of antennas A, A_1, and A_2.

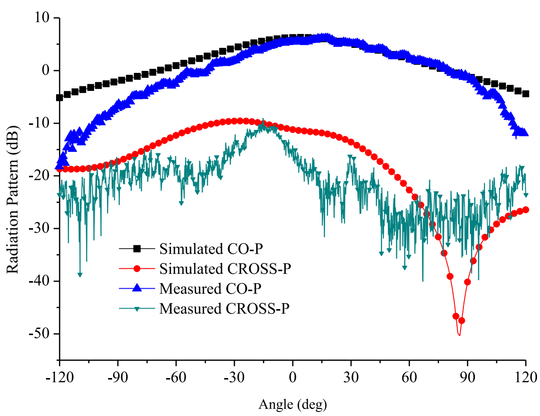

Fig. 10. Measured radiation pattern of antenna A of 25.3 GHz.

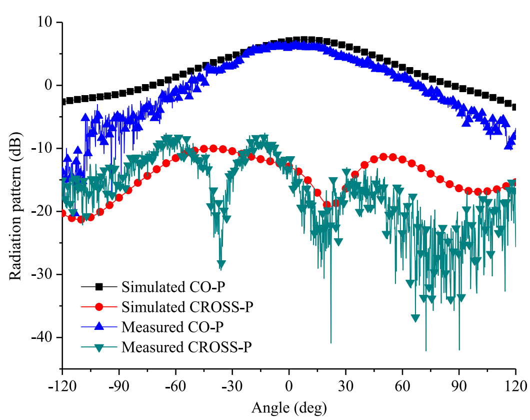

Fig. 11. Measured radiation pattern of antenna A of 30.76 GHz.

25.3 to 30.7 GHz, which shows the possibility of the frequency differences adjustment. Figs. 10 and 11 depict the simulated and measured radiation patterns of the antenna A with gain greater than 6 dBi on both frequency points.

IV. Conclusion

A detailed analysis of a novel Ka-band dual-frequency single-slot antenna based on an SIW structure is demonstrated in this letter. The proposed design starts from the view of the SIW resonator to obtain the performance of dual frequency in the single-slot antenna. The single slot disturbs the current distributions of TE_{101} and TE_{102} modes at the same time, then radiates the energy. The proposed antennas resonate within the frequency range from 25.3 to 30.7 GHz with gain greater than 6 dBi according to the measured results. Moreover, the frequency differences may be adjusted by changing the length of the SIW structure. Realizing the dual-frequency characteristic in a single-slot antenna has a bright future in antenna minimization in millimeter-wave range.

References

[1] C. W. James, "Status of millimeter wave technology and applications in the US," in *Proc. 21st Eur. Microw. Conf.*, Oct. 1991, vol. 1, pp. 150–157.

[2] J. Hasch, E. Topak, R. Schnabel, T. Zwick, R. Weigel, and C. Waldschmidt, "A millimeter-wave technology for automotive radar sensors in the 77 GHz frequency band," *IEEE Trans. Microw. Theory Techn.*, vol. 60, no. 3, pp. 845–860, Mar. 2012.

[3] W. Jiang, C. Liu, B. Zhang, and W. Menzel, "K-band frequency-scanned leaky-wave antenna based on composite right/left-handed transmission lines," *IEEE Antennas Wireless Propag. Lett.*, vol. 12, pp. 1133–1136, 2013.

[4] J. Burns, "The application of millimeter wave technology for personal communication networks in the United Kingdom and Europe: A technical and regulatory overview," in *IEEE MTT-S Int. Microw. Symp. Dig.*, May 1994, vol. 2, pp. 635–638.

[5] Y. C. Lee and J. S. Sun, "Compact printed slot antennas for wireless dual- and multi band operations," *Prog. Electromagn. Res.*, vol. 88, pp. 289–305, 2008.

[6] W. Menzel and A. Moebius, "Antenna concepts for millimeter-wave automotive radar sensors," *Proc. IEEE*, vol. 100, no. 7, pp. 2372–2379, Jul. 2012.

[7] J. Janapsatya and K. P. Esselle, "Multi-band WLAN antennas based on the principle of duality," in *Proc. IEEE APS Int. Symp.*, Jul. 2006, pp. 2679–2682.

[8] T. Hongnara, C. Mahattanajatuphat, P. Akkaraekthalin, and M. Krairiksh, "A multiband cpw-fed slot antenna with fractal stub and parasitic line," *Radio Eng.*, vol. 21, no. 2, pp. 597–605, Jun. 2012.

[9] A. P. Saghati and K. Entesari, "A reconfigurable SIW cavity-backed slot antenna with one octave tuning range," *IEEE Trans. Antennas Propag.*, vol. 61, no. 8, pp. 3937–3945, Aug. 2013.

[10] T. Li, H. Meng, and W. Dou, "Design and implementation of dual-frequency dual-polarization slotted waveguide antenna array for ka-band application," *IEEE Antennas Wireless Propag. Lett.*, vol. 13, pp. 1317–1320, 2014.

[11] R. De, B. B. Chowdhury, and M. Bhowmik, "A novel design of dual frequency SIW slot antenna," in *Proc. 23rd Int. Conf. Signal Process. Integr. Netw.*, Feb. 2016, 11–12.

[12] S. Chang, Y. Li, and X. Yang, "A dual-frequency antenna for WLAN/WiMAX applications," *Appl. Sci. Technol.*, vol. 6, pp. 20–24, 2011.

[13] M. Bozzi, A. Georgiadis, and K. Wu, "Review of substrate-integrated waveguide circuits and antenna," *Microw., Antennas Propag.*, vol. 5, no. 8, pp. 909–920, 2011.

[14] F. Xu and K. Wu, "Guided-wave and leakage characteristics of substrate integrated waveguide," *IEEE Trans. Microw. Theory Techn.*, vol. 53, no. 1, pp. 66–73, Jan. 2005.

[15] N. Chahat, R. Hodges, J. Sauder, M. Thomson, E. Peral, and Y. Rahmat-Samii, "CubeSat deployable Ka-band mesh reflector antenna development for earth science missions," *IEEE Trans. Antennas Propag.*, vol. 64, no. 6, pp. 2083–2091, Jun. 2016.

[16] J. Wang, L. Yu, and R. Zhao, "Antenna performance measurements on Ku and Ka bands for TM65m radio telescope," in *Proc. IEEE Int. Conf. Microw. Millim. Wave Technol.*, 2016, pp. 6–10.

[17] A. Krauss, H. Bayer, R. Stephan, and M. Hein, "Dual-band leaky-wave antenna based on a dual-layer frequency selective surface for bi-directional satcom-on-the-move in Ka-band," in *Proc. Int. Workshop Antenna Technol.*, 2016, pp. 25–28.

[18] A. Farrall and P. Young, "Integrated waveguide slot antennas," *Electron. Lett.*, vol. 40, no. 16, pp. 974–975, Aug. 2004.